20th International Conference on Structural Mechanics in Reactor Technology (SMiRT 20)
Espoo, Finland, August 9-14, 2009
SMiRT 20-Division 5, Paper 1819

Response of Conventional and Base-Isolated Nuclear Power Plants to Blast Loading

Yin-Nan Huang[a] and Andrew S. Whittaker[b]

[a]*School of Civil and Environmental Engineering, Assistant Professor, Nanyang Technological University, Singapore, e-mail: YNHuang@ntu.edu.sg*
[b]*University at Buffalo, Buffalo, New York, USA*

Keywords: Air blast, ground shock, base isolation, nuclear power plant, hydrocode.

1 ABSTRACT

This paper summarizes a study that assesses the performance of sample conventional and base-isolated reactor buildings under blast loadings, including air blast and blast-induced ground shock. The blast assessment of the sample reactor building is performed for an assumed threat of 2000 kg of TNT explosive detonated on the surface with a distance to the reactor building of 10 m. The air- and ground-shock waves produced by the design threat are generated and used for performance assessment. The air-blast loading on the sample reactor building is computed using a Computational Fluid Dynamics code, Air3D, and the ground-shock time series is generated using an attenuation model for rock response. Response-history analysis of the sample conventional and base isolated reactor buildings to external blast loadings is performed using LS-DYNA. The structural responses, including acceleration, drift and peak floor acceleration demands on key secondary systems attached to the internal structure of the reactor building are identified for both the conventional and base-isolated sample NPP. The results show that the installation of base isolation systems does not increase the vulnerability of the containment vessel to air-blast loading and reduces the ground-shock response by orders of magnitude.

2 INTRODUCTION

Safety-related nuclear facilities are required by code and regulations to be designed for a family of extreme events, including very rare earthquake shaking, loss of coolant accidents, and tornado-borne missile impacts. The terrorist attacks of September 11, 2001, added another extreme event to the family, namely, attack by improvised explosive devices, military munitions and airplanes.

Base isolation systems have been widely used to protect mission-critical infrastructure from earthquake -induced damage. More than 3000 buildings, bridges and other types of infrastructure have been base isolated to date, including six applications to nuclear power plants (NPPs): four in France and two in South Africa (Buckle et al. 1987). Although the seismic response of base-isolated structures has been carefully investigated and well documented (e.g., Naeim and Kelly 1999; Constantinou et al. 2007), the response of base-isolated structures to blast loading has neither been studied nor documented to the knowledge of the authors. This paper summarizes a study that identifies the impact of the implementation of *seismic* isolation systems on the *blast* vulnerability of a sample NPP reactor building. Additional information is available in (Huang et al. 2008, 2009).

The study summarized in this paper considered air-blast and ground-shock loadings from conventional improvised explosive devices only. Loadings associated with the detonation of thermonuclear weapons, terrorist attack of reactor buildings through the use of aircraft similar to the attacks of 9/11/2001, and malevolent acts against reactor buildings using military munitions are not addressed.

The effects of external air-blast loadings and blast-induced ground shock on structures should be assessed using global and local response metrics. An important global response metric is collapse. Collapse of a continuum such as a reinforced concrete containment vessel is extremely unlikely and could only result from the destruction of much of the containment vessel, which would result in egregious damage to and likely failure of the internal structure and secondary systems. Local response metrics for reinforced concrete elements are spalling and breach. Spalling of concrete is a result of the reflection of shock-induced compressive waves off the rear surface of a reinforced concrete component. Breach results from the gross

spalling of concrete such that a clear passage is opened from the front surface of the concrete to the rear surface. The introduction of seismic isolation bearings below a reactor building will not impact the likelihood of spalling and/or breaching of the structure. In the study presented herein, global responses are measured using roof displacement and base shear of the containment vessel and base shear of the internal structure. Local responses are measured using peak floor accelerations at the supports of the reactor assembly and a steam generator. The global and local responses of the conventional (fixed base) and base-isolated reactor buildings are computed and compared to identify the impact of the base isolation systems on the blast-induced response of the sample NPP.

A Computational Fluid Dynamics (CFD) code and empirical attenuation relationships were used to generate loading histories of air and ground shock, respectively. A CFD code was used for the air shock calculations because the widely used simplified procedures, such as the equivalent single degree of freedom analysis, are incapable of capturing the complex loading environment associated with a conventional weapons detonation at a standoff distance of less than the diameter of the containment vessel.

Numerical models of the conventional and isolated reactor buildings were developed and analyzed using the hydrocode LS-DYNA (LSTC 2003) to compute the global and local responses of the sample reactor building subjected to air- and ground-shock loadings. The air- and ground-shock loadings were de-coupled: the air shock analysis assumes that the explosive is detonated on a near-rigid reflecting surface producing only limited ground shock and a small crater and the base slab of the reactor building is assumed to be rigid and fixed to the subgrade; the ground-shock analysis assumes that the detonation results in ground shock and no air shock. A fully coupled hydrocode analysis involving a numerical model of the air, rock/soil and reactor building would be required to correctly partition the explosive effects between air and ground shock. Such analysis was not attempted as the goal was to assess the impact of isolating the reactor building on its vulnerability to blast loadings, rather than the energy partition between air and ground shock for a given blast scenario.

Four sections follow this introduction. Section 3 introduces the sample conventional and base-isolated reactor building and the numerical models used in the hydrocode (LS-DYNA) analyses. Section 4 introduces the target threat (weapon size and standoff distance) for the assessment of the sample reactor building as well as the histories of air-blast pressure and ground shock developed for the target blast threat. Section 5 presents the results of the hydrocode analysis of the conventional and isolated reactor building subjected to the air pressure and ground-shock histories of Section 4. Section 6 discusses the impact of seismic isolation on the blast vulnerability of the sample reactor building and provides directions for future research.

3 SAMPLE REACTOR BUILDING

Figure 1 shows a cutaway view of the sample NPP reactor building of conventional construction. The sample reactor building consists of a containment vessel and an internal structure to which the key secondary systems of the NPP, including the reactor and steam generators, are attached. The heights of the containment vessel and internal structure are 61 and 39 meters, respectively. The diameter of the containment vessel is 42 meters. The total weight of the NPP reactor building is approximately 75,000 tons.

Panels a and b of Figure 2 present the numerical models developed in LS-DYNA for the containment vessel and internal structure, respectively. The containment vessel was modelled using 3584 four-node shell elements, of which 1024 were used for the base slab and 2560 were used for the dome and the wall. Elastic material properties were assigned to the shell elements. The first mode period of the model for the containment vessel is approximately 0.2 second. The internal structure of the sample reactor building was modelled as a lumped-mass stick. The mass of the primary (structural) and secondary (or non-structural) components of the internal structure was lumped at discrete nodes on the stick. The reactor and one steam generator were supported at Nodes 1 and 2 of Figure 2b, respectively. Elastic beam elements were used for the stick model because preliminary simulations indicated that the shearing force demands produced by the blast loadings were much smaller than the shearing strength of the structural components in the internal structure. The mechanical properties of the beam element that composes each stick were provided by the supplier of the sample NPP. The properties were back-calculated from a 3D model of the reactor building. The first mode period of the model for the internal structure is approximately 0.14 second.

To develop the finite element model for the base-isolated reactor building, bilinear springs were placed beneath the base slab of the conventional reactor building. The nonlinear force-displacement relationship for the springs used in the model, presented in Figure 3, represents the hysteretic behavior of lead-rubber

bearings. The period associated with the second-slope stiffness was assigned a value of 2 seconds. In the LS-DYNA model of the base-isolated reactor building, the bilinear spring of Figure 3 was modelled using a beam element and the *nonlinear plastic discrete beam* material model, which can capture the effects of elasto-plastic behavior using six springs, one for each of the six local degrees of freedom.

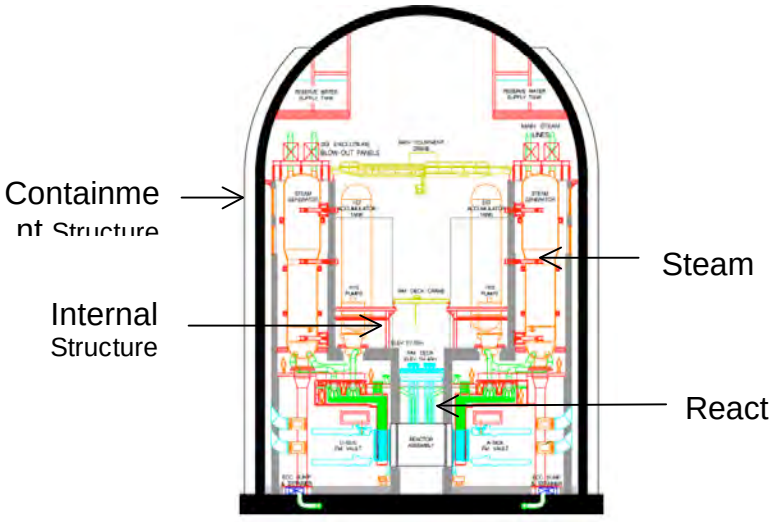

Figure 1. Cutaway view of the sample NPP reactor building

a. Containment vessel b. Lumped-mass stick for the internal structure

Figure 2. LS-DYNA model for the conventional NPP reactor building

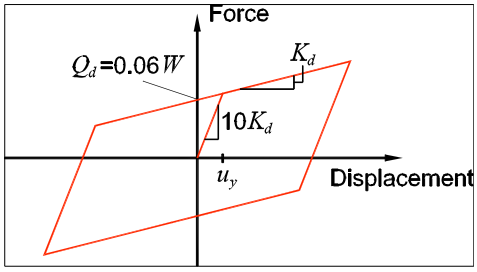

Figure 3. Assumed properties of the LR bearings

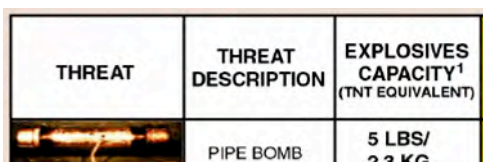

4 BLAST LOADINGS

4.1 Blast threat

This study considered blast loading using conventional improvised explosive devices. In the United States, the Federal Bureau of Investigation (FBI) has the lead responsibility for dealing with terrorism. The scale of improvised explosive devices spans many orders of magnitude. The Technical Services Working Group (TSWG) developed a threat chart, which is reproduced in part in Figure 4. Hand-delivered explosives range in size from a few pounds to 23 kg. Vehicle-borne threats can range in size up to 27,000 kg of explosive.

The design blast hazard for the response-history analysis performed herein was determined using the threat chart of Figure 4. The likelihood of a great weight of truck- or trailer-borne explosive to be detonated close to a NPP reactor building is extremely low due to the strict security employed at nuclear power plants. The threat assumed for the assessment reported below was 2000 kg of hemispherical TNT detonated on the ground surface, 10 m from the face of the sample reactor building. Figure 5 illustrates the analysis.

For the purpose of data presentation, six points (A through F) are identified in Figure 5. Point A is at the top of the dome of the reactor building and Point B is at the center of the base slab, directly below Point A. Point D is at the base of the reactor building at the closest point on the containment vessel to the detonation. Point C is 40 m above Point D. Points E and F are at the base of the containment vessel, 90 and 180 degrees rotated from Point D, respectively.

Figure 4. TSWG threat chart

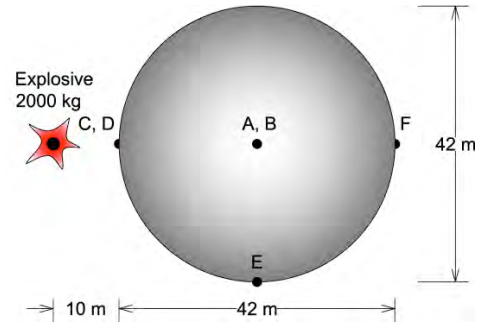

a. Plan view

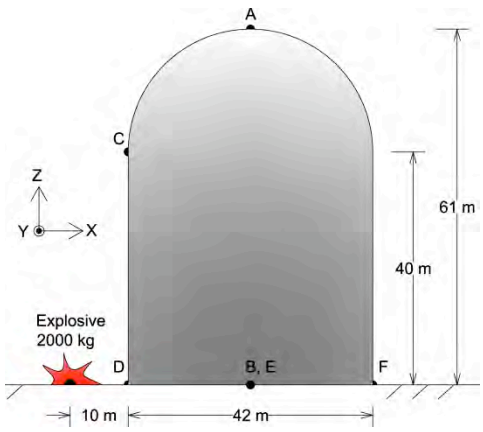

b. Elevation view

Figure 5. Layout of the blast analysis

4.2 Air blast

The reflected pressure histories on the surface of the containment vessel were computed using the CFD code, Air3D (Rose 2006), which solves the Eulerian conservation equations (momentum, mass and energy) in three dimensions. Rose (2006) provdies comprehensive information on the numerical strategies adopted in Air3D.

A numerical model was developed in Air3D including the 2000-kg TNT explosive and the sample containment vessel. The exterior surface of the containment vessel was covered with 2560 pressure monitoring points, one per shell element of the LS-DYNA model of the vessel. The location of each monitoring point in the Air3D model was set equal to the center of the corresponding shell element in the LS-DYNA model. Each monitoring point yielded a pressure history for the response-history analysis of the vessel.

Figure 6 presents the pressure histories at Point D, C and A on the containment vessel (see Figure 5b) for the assumed blast threat. The peak reflected pressure drops rapidly as the distance and angle of incidence from the explosive to the monitoring point increase. The peak pressures at Points D, C and A were 7890, 207 and 22 kPa, respectively. The arrival time of the pressure at Points D, C and A are 3.8, 40.0 and 118.5 msec, respectively. The positive pressure loading at Point D vanishes before the shock wave reaches Point C, 40 m above Point D. The positive pressure loading at Point C vanishes before the shock wave reaches Point A. Figure 7 presents the pressure contour plots of the Air3D analysis for the sample containment vessel and the assumed threat at 18 msec after the explosive was detonated. At t = 18 msec, the shock wave distributes between the elevations of 8 and 27 m above the ground at the cutaway section of Figure 7. The positive overpressure at Point D has diminished substantially before the shock wave reaches Point C.

The simplified procedures that are widely used for the blast design of structures cannot capture the interaction of shock waves and complex geometries or the effect of different shock wave arrival times on

global and local structural responses. The complex loading environment studied herein and the resultant structural responses can only be understood using CFD tools and response-history analysis.

Figure 8 presents the translational load history on the containment vessel in the X direction. This history was computed as the sum of the X components of the force histories acting on the 2560 shell elements at every step in the time series; the arrival time of the shock wave at each monitoring location was preserved. The peak translational load and positive phase impulse of Figure 8 are 3.13×10^5 kN (6 msec after detonation) and 4.85×10^6 kN-msec, respectively.

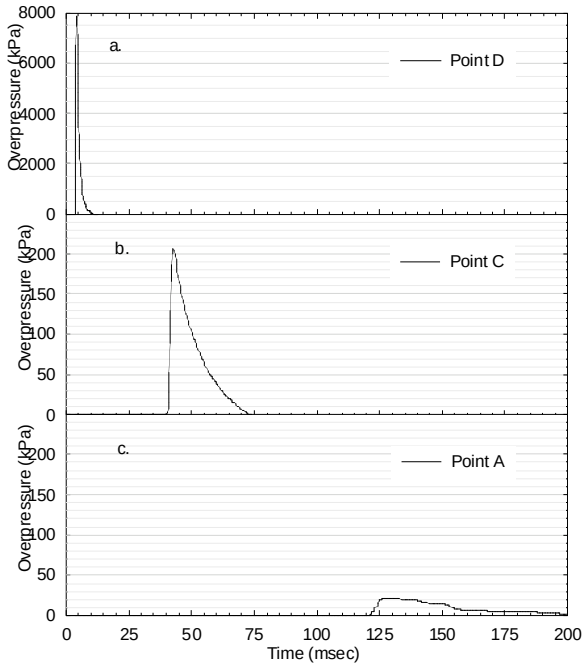

Figure 6. Pressure histories at Points A, C and D of Figure 5 for the air-blast analysis of the sample NPP

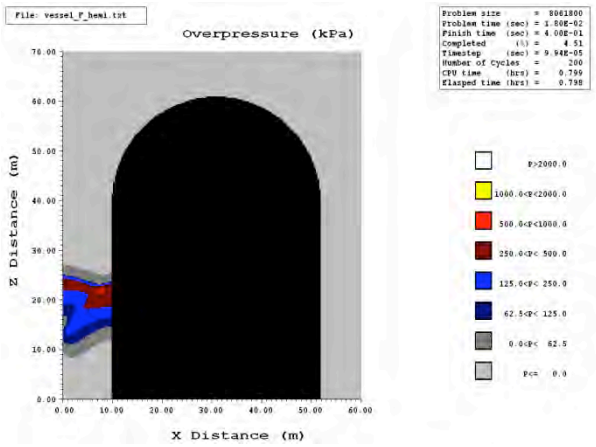

Figure 7. Pressure contour plots for the Air-3D analysis at the instant of 18 msec after detonation

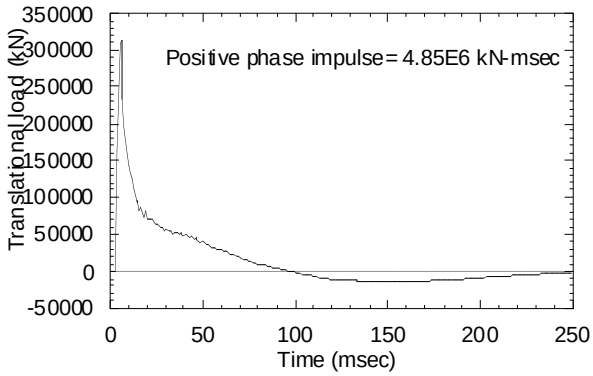

Figure 8. Translational load history for the air-blast analysis of the sample NPP

4.3 Ground shock

An acceleration time series was generated using the recommendations of Wu and Hao (2005) to simulate the ground shock introduced by the blast threat. Wu and Hao (2005) modeled simultaneous ground and air shock generated by surface explosions. They developed a numerical model to simulate the response of granitic rock to explosive loading and validated the model using field test results. Hydrocode models of air, granite and TNT were developed to simulate the ground shock and air-blast pressure histories for different blast threats. Instead of providing attenuation relationships for peak particle displacement (PPD) and peak particle velocity (PPV) such as those of Westine (1978), TM5-1300 (DoA 1991) and Smith and Hetherington (1994), Wu and

Hao developed empirical relationships using the simulation data for parameters that they considered essential for developing ground-shock acceleration histories, including arrival time, peak particle acceleration (PPA), load duration, the shape of the time series and the power spectrum of the ground shock.

The intensity of the ground shock diminishes rapidly with distance, with amplitude at Point D (10 m from the detonation) being much greater than that on the opposite side of the containment vessel, 52 m from the detonation. For this study, an averaged distance of 31 m, equal to the distance between the point of detonation and the center of the base slab (Point B), was used for ground shock simulation. Figure 9 presents the resultant acceleration history. More information for the development of the acceleration history of Figure 9 is provided in Huang et al. (2008, 2009).

The attenuation model of Wu and Hao (2005) was used to determine the ground shock parameters since it provides sufficient information for simulating a ground acceleration history. The values of PPA, PPV and PPD associated with the acceleration history of Figure 9 are 93.2 g, 0.38 m/s and 0.00038 m[1], respectively. As a point of reference, the values of PPA, PPV and PPD recommended inTM5-1300 for a surface detonation of 2000 kg of explosive at a distance of 31 m are 15.9 g, 0.25 m/s and 0.013 m, respectively. The values of PPV and PPD predicted using Westine (1978) with a scaled factor of 0.4 to consider coupling between the explosive and the ground are 0.54 m/s and 0.00078 m, respectively. The significant difference in the predictions between models indicates the need for additional study to enable predictions of key soil response parameters for analysis of ground shock due to surface detonations.

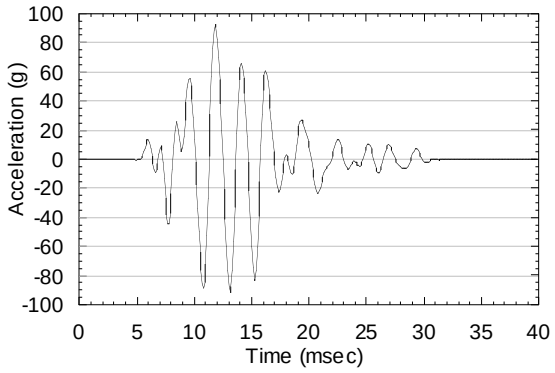

Figure 9. Acceleration history used in the ground-shock analysis of the sample reactor buildings

5 STRUCTURAL RESPONSES

5.1 Air blast

This subsection presents the results of the air-blast analysis. Global responses (drift and base shear for the containment vessel and base shear for the internal structure) and local responses (peak floor acceleration at Nodes 1 and 2 of Figure 2b) are reported for the conventional and base-isolated reactor buildings. Since the internal structure of the conventional reactor building is well-protected from the air-blast loading, the discussion of local responses focuses on the base-isolated reactor building only.

Figure 10 presents the base shear histories for the conventional and base-isolated containment vessel subjected to the air-blast loading of Section 4. The peak base shear force in the conventional containment vessel is 125,000 kN (51% of the total weight of the containment vessel without the base slab, $0.51W_{con}$), which occurred at 5.7 msec, and very close to the time of the peak translational load (see Figure 8). The peak base shear for the base-isolated containment vessel is 115,000 kN ($0.47W_{con}$): 92% of the peak base shear for the conventional reactor building. The peak base shear force for the internal structure in the base-isolated reactor building is 86,000 kN (37% of the total weight of the internal structure, $0.37W_{int}$). As a point of reference, the shear strengths at the base of the containment vessel and internal structure are 483,000 kN and

[1] The acceleration history of Figure 9 was integrated with respect to time for the velocity and displacement histories, where the peak values were identified as PPV and PPD, respectively.

327,000 kN, respectively[2]. The peak drift between Points A and B for the conventional and base-isolated reactor buildings subjected to the air-blast loading of Section 4 are 6 and 4 mm, respectively. The peak global responses of this subsection are tabulated in the second last row of Table 1.

Figure 11 presents the acceleration histories at Nodes 1 and 2 of Figure 2b. The peak accelerations at Nodes 1 and 2 are 0.24 and 0.4 g, respectively. As another point of reference, the peak floor accelerations at Nodes 1 and 2 for the sample conventional reactor building subjected to the Safe Shutdown Earthquake (SSE) established for an uniform risk (specifically, an annual probability of exceedance of unacceptable performance) of 10^{-5} are in the range of 0.6 to 0.8 g; see Huang et al. (2008) for more information.

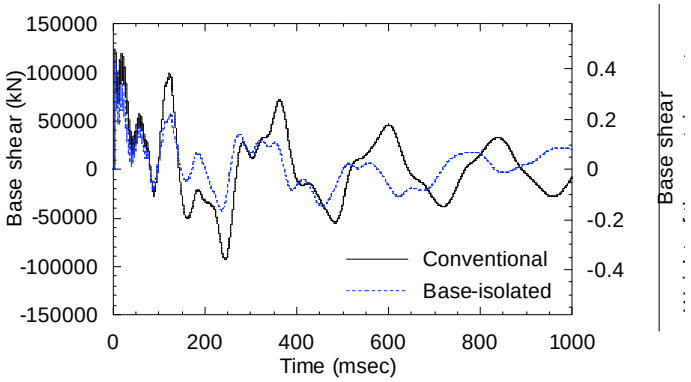

Figure 10. Base shear histories for the conventional and base-isolated containment vessel subjected to the air-blast loading of Section 4

Table 1. Drifts and base shears of the conventional and base-isolated reactor buildings subjected to the air-blast and ground-shock loadings of Section 4

Loading type	Roof drift (mm)		Base shear (kN)			
			Containment vessel		Internal structure	
	Conventional	Base-isolated	Conventional	Base-isolated	Conventional	Base-isolated
Air blast	6.0	4.0	125000	115000	0	86000
Ground shock	0.38	0.02	637000	410	69800	415

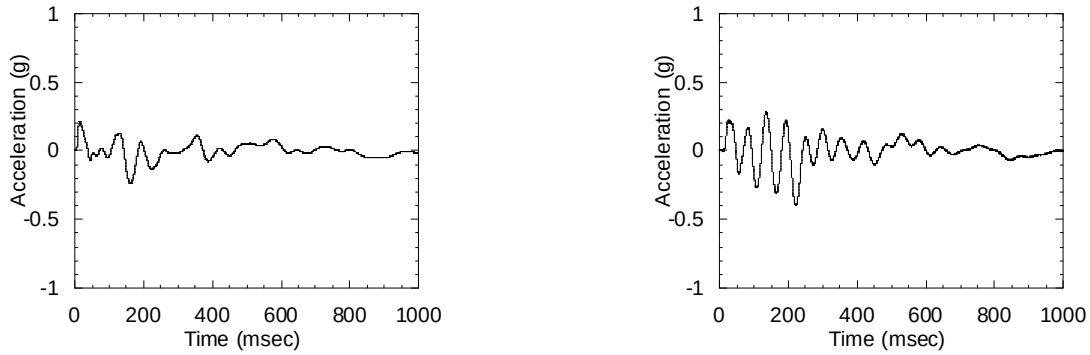

[2] The shear strengths were computed using $0.5\sqrt{f_c'}A_S$, where f_c' is the compressive strength of concrete and a value of 35 N/mm^2 was used in this study and A_S is the shear area of each internal-structure stick in mm^2 provided by the supplier of the sample NPP.

a. Node 1 b. Node 2

Figure 11. Acceleration histories at Nodes 1 and 2 Nodes 1 and 2 of Figure 2b for the base-isolated reactor building subjected to the air-blast loading of Section 4

5.2 Ground shock

The peak values of the global responses for the conventional and base-isolated reactor buildings subjected to the ground shock of Figure 9 are listed in the last row of Table 1. Panels a and b of Figure 12 present the base shear histories for the conventional and base-isolated reactor buildings, respectively, subjected to the ground shock of Figure 9. Reductions by orders of magnitude are the result of the addition of the base-isolaton system.

Figure 12a shows that the peak base shear in the conventional containment vessel is more than twice its reactive weight, which is not a surprising result since the ground-shock history had a PPA of 93.2 g (see Figure 9). These results need to be interpreted with caution because 1) studies are needed to verify the reliability of the ground shock model used in this study, 2) the assumption of elastic response for a base shear of twice the reactive weight may not be valid, 3) the effects of vertical shaking due to ground shock have not been considered, and 4) the ground shock effects were considered as an in-phase loading at all support points beneath the base slab, rather than as a traveling wave, with an amplitude equal to that computed for the center of the base slab.

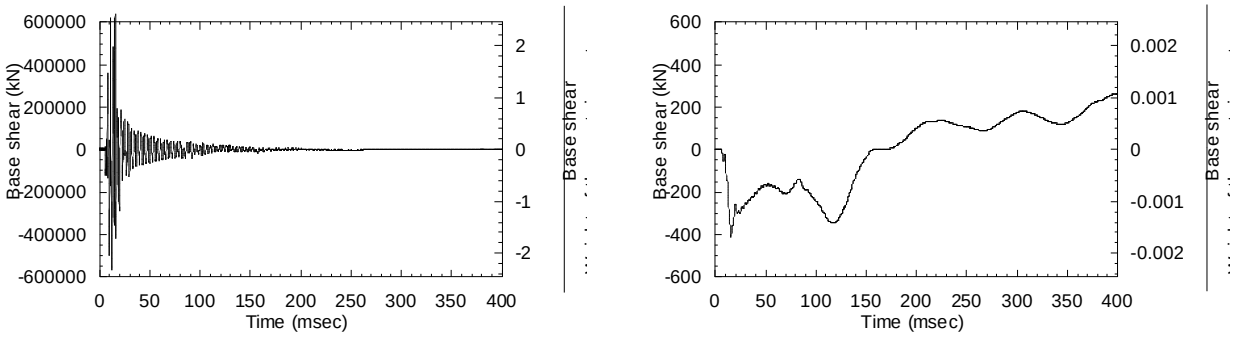

a. Conventional b. Base-isolated

Figure 12. Base shear histories for the conventional and base-isolated containment vessel subjected to the ground shock of Figure 9

Figure 13 presents the acceleration histories at Nodes 1 and 2 of Figure 2b for the conventional and base-isolated reactor buildings subjected to the ground shock of Figure 9. The peak accelerations of the four time series of Figure 13 are tabulated in Table 2. The demands on the secondary systems for the base-isolated NPP are much smaller than those for the conventional reactor building. The isolation systems were extremely effective at filtering out high frequency ground-shock loading.

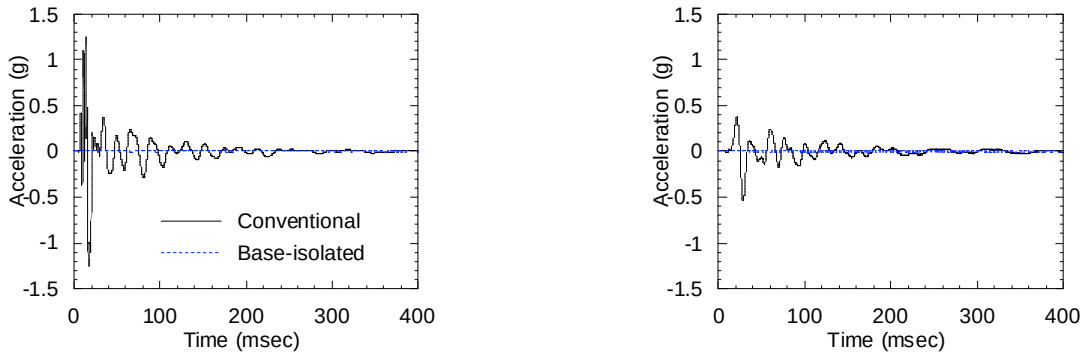

a. Node 1 b. Node 2

Figure 13. Acceleration histories at Nodes 1 and 2 Nodes 1 and 2 of Figure 2b for the conventional and base-isolated reactor buildings subjected to the ground shock of Figure 9

Table 2. Peak floor accelerations at Nodes 1 and 2 for the conventional and base-isolated reactor buildings subjected to the ground shock of Figure 9

Response	Loading type	Structural system	Node 1	Node 2
Peak floor acceleration (g)	Ground shock	Conventional	1.26	0.54
		Base-isolated	0.007	0.011

6 CLOSING REMARKS

The analysis results presented in this paper show that the installation of base isolation does not increase the vulnerability of the sample NPP reactor building to air-blast loading and greatly improves the performance of the containment and internal structures subjected to ground shock. For air-blast analysis, the base-isolated containment vessel had a smaller base shear and roof drift than the conventional containment vessel. The secondary systems attached to the internal structure in the base-isolated NPP experienced relatively low floor acceleration demands, associated with extremely small probabilities of failure. The non-isolated containment vessel protected the secondary systems attached to the internal structure from the effects of air-blast loading (in part due to the assumption of base slab rigidity and restraint). For ground-shock analysis, the implementation of the isolators reduced the global and local responses by orders of magnitude.

The study presented herein was limited by a family of assumptions that were identified in Sections 2 through 5. Further research is needed to a) characterize the partitioning of blast induced energy between air and ground shock, and b) develop and validate by field experiments robust procedures to generate horizontal and vertical acceleration time series due to ground shock for common types of soils, clays and rock.

Acknowledgements. *The research presented herein was supported in part by MCEER through grants from the Earthquake Engineering Centers Program of the National Science Foundation (NSF), Award Number EEC-9701471, and the State of New York. The opinions expressed in report are those of the authors and do not reflect the views of the sponsors, the Research Foundation of the State University of New York.*

Dr. Ayman Saudy and Mr. Medhat Elgohary of Atomic Energy Canada Limited (AECL) provided valuable information on NPP reactor building construction. Mr. Graeme Ballantyne of Thornton-Tomasetti, San Francisco, helped develop a finite element model for the sample containment vessel. Dr. Timothy Rose, formerly of Cranfield University, generously provided his CFD code, Air3D, for the air-blast computations. The authors gratefully acknowledge their assistance.

REFERENCES

Buckle, I. G., Kelly, T. E., and Jones, L. R. (1987). "Basic concepts of seismic isolation and their application to nuclear structures." in *Seismic Engineering: Recent Advances in Design, Analysis, Testing and Qualification Methods*, American Society of Mechanical Engineers, PVP-Vol 127, 429-437.

Constantinou, M. C., Whittaker, A. S., Kalpakidis, Y., Fenz, D. M., and Warn, G. P. (2007) "Performance of seismic isolation hardware under service and seismic loading." *MCEER-07-0012*, Multidisciplinary Center for Earthquake Engineering Research, State University of New York, Buffalo, NY.

Department of the Army (DoA). (1990). "Structures to resist the effects of accidental explosions." *Army TM 5-1300*, U.S. Department of the Army, Washington, D.C.

Huang, Y.-N., Whittaker, A. S., and Luco, N. (2008). "Performance assessment of conventional and base-isolated nuclear power plants for earthquake and blast loadings." *MCEER-08-0019*, Multidisciplinary Center for Earthquake Engineering Research, State University of New York, Buffalo, NY.

Huang, Y.-N., Whittaker, A. S. and Ballantyne, G. (2009) "Vulnerability assessment of conventional and base-isolated nuclear power plants for blast loadings." Paper in preparation, *Nuclear Engineering and Design*.

Naeim, F., and Kelly, J. M. (1999). *Design of seismic isolated structures: from theory to practice*, John Wiley, NY.

Rose, T. A. (2006). *A computational tool for airblast calculations -- Air3d version 9 users' guide*, Engineering Systems Department, Cranfield University, Shrivenham, United Kingdom.

Smith, P. D., and Hetherington, H. J. (1994). *Blast and ballistic loading of structures*, Butterworth-Heinemann, Oxford, United Kingdom.

Westine, P. S. (1978). "Ground shock from the detonation of buried explosives." *Journal of Terramechanics*, 15(2), 69-79.

Wu, C., and Hao, H. (2005). "Modeling of simultaneous ground shock and airblast pressure on nearby structures from surface explosions." *International Journal of Impact Engineering*, 31(6), 699-717.